ORNL/NRC/LTR-00/02

Contract Program or Project Title:	Heavy-Section Steel Technology (HSST) Program Engineering Technology Division
Subject of this Document:	Application of Statistically-Based K_{Ic}/K_{Ia} Fracture Toughness Models to PTS Assessments of Reactor Pressure Vessels
Type of Document:	Letter Report
Authors:	B. R. Bass T. L. Dickson P. T. Williams
Date Published:	April 2000
Responsible NRC Individual and NRC Office or Division	M. T. Kirk Division of Engineering Technology Office of Nuclear Regulatory Research

Prepared for the
U. S. Nuclear Regulatory Commission
Washington, D.C. 20555-0001
Under Interagency Agreement DOE 1886-N011-9B
NRC JCN No. B0119

OAK RIDGE NATIONAL LABORATORY
Oak Ridge, Tennessee 37831-8056
managed and operated by
UT-Battelle, LLC
for the
U. S. DEPARTMENT OF ENERGY
under Contract No. DE-AC05-00OR22725

ORNL/NRC/LTR-00/02

Application of Statistically-Based K_{Ic}/K_{Ia} Fracture Toughness Models to PTS Assessments of Reactor Pressure Vessels

B. R. Bass

T. L. Dickson

P. T. Williams

Oak Ridge National Laboratory

Oak Ridge, Tennessee

Manuscript Completed – January 2000
Date Published – April 2000

Prepared for the
U.S. Nuclear Regulatory Commission
Office of Nuclear Regulatory Research
Under Interagency Agreement DOE 1886-N011-9B

NRC JCN No. B0119

OAK RIDGE NATIONAL LABORATORY
Oak Ridge, Tennessee 37831-8063
managed and operated by
UT-Battelle
for the
U.S. DEPARTMENT OF ENERGY
under Contract No. DE-AC05-00OR22725

Application of Statistically-Based K_{Ic}/K_{Ia} Fracture Toughness Models to PTS Assessments of Reactor Pressure Vessels

B. R. Bass, T. L. Dickson, and P. T. Williams

Oak Ridge National Laboratory
P. O. Box 2009
Oak Ridge, TN, 37831-8056

ABSTRACT: The Heavy-Section Steel Technology (HSST) Program at ORNL has developed new statistical representations of extended fracture toughness K_{Ic} and K_{Ia} databases for reactor pressure vessel (RPV) steels. A 2-parameter Weibull distribution, with the parameters calculated by the *Method of Moments* point-estimation technique, forms the basis for the new statistical models. This report describes applications of the new ORNL statistical models, as implemented in the FAVOR probabilistic fracture mechanics program, to pressurized-thermal-shock (PTS) assessments of selected RPVs. Fracture initiation and failure probabilities computed with the FAVOR implementation for certain PTS scenarios are compared to those generated using the current methodology based on the Integrated Pressure-Thermal-Shock (IPTS) studies of the mid-1980s. Differences between probabilities of vessel failure predicted using the ORNL and IPTS representations of K_{Ic} and K_{Ia} are shown to depend on characteristics of the PTS transient and the embrittlement of the RPV.

1. Introduction

The HSST Program at ORNL has produced new statistical representations of available data for the properties of plane-strain static initiation toughness, K_{Ic}, and plane-strain crack-arrest toughness, K_{Ia}, used to characterize the fracture toughness of reactor pressure vessel (RPV) steels [1]. This effort was performed in the context of a probabilistic methodology appropriate for use in an overall effort by the Nuclear Regulatory Commission (NRC) to update its regulatory guidance for pressurized-thermal-shock (PTS) transients. These new representations for K_{Ic} and K_{Ia} were developed through the application of rigorous mathematical procedures applied to an extended fracture toughness database for RPV steels. The procedures relied on a purely statistical approach and did not distinguish between the aleatoric (randomness) and epistemic (state of

knowledge) uncertainties in the database.[1] However, the ORNL models for K_{Ic} and K_{Ia} do provide a statistically-derived alternative to current PTS assessment methodology that was introduced during the NRC-sponsored Integrated Pressurized-Thermal-Shock (IPTS) studies performed in the mid-1980s [2-3]. A complete description of the technical bases for the ORNL statistical representations of the extended K_{Ic} and K_{Ia} databases is provided in Ref. [1].

This report describes applications of the new ORNL K_{Ic} and K_{Ia} statistical models, as implemented in the FAVOR probabilistic fracture mechanics program [4], to pressurized-thermal-shock (PTS) assessments of selected RPVs. Section 2 provides a description of the extended K_{Ic} and K_{Ia} databases used to generate the new statistical models. In Section 3, the K_{Ic} and K_{Ia} statistical models derived in Ref. [1] are summarized in both graphical and analytical form. In Section 4, the FAVOR implementation of the new statistical models is applied to selected PTS assessments of RPVs, and the results are compared to those generated using the current IPTS-based methodology. Some conclusions derived from these comparative analyses are given in Section 5.

2. Extended K_{Ic} And K_{Ia} Databases

In support of the NRC effort to update PTS regulatory procedures, ORNL conducted a survey to identify K_{Ic} data from pressure vessel steels to augment the EPRI fracture toughness database [5] as amended by Nanstad et al. [6]. The candidate K_{Ic} data were evaluated using specific requirements that included the following: (a) satisfaction of validity requirements given in ASTM Standard E 399 [7], (b) availability in tabular form, and (c) availability of the reference nil-ductility transition temperature (RT_{NDT}) determined according to ASME Boiler and Pressure Vessel Code requirements [8]. A similar survey was carried out to compile an extended K_{Ia} database that would include those data given in the EPRI report [5]. Because the ASTM Standard E 1221 [9] for K_{Ia} is relatively new, many of the existing data were generated prior to adoption of this standard. Thus, it was agreed that candidate K_{Ia} data would be evaluated in a more general

[1] Accounting for aleatoric and epistemic uncertainties in the formulation of new fracture toughness models is being emphasized in current NRC development of probabilistic risk assessment (PRA) methodology for PTS regulation. In support of that effort, on-going studies at the University of Maryland are distinguishing between these uncertainties in the context of a physically-based approach to the modeling of fracture toughness.

context, including engineering judgment of acknowledged experts and general acceptance by the nuclear technology community.

2.1 K_{Ic} Database

In 1978, the ASME Section XI Task Group on Flaw Evaluation published an EPRI report [5] that includes the experimental fracture toughness data used in the construction of the ASME K_{Ic} and K_{Ia} curves. In 1993, Nanstad et al. [6] at ORNL carried out a study to review the technical bases applied in the establishment of the ASME K_{Ic} curve. That study compared the data reported in Refs. [5, 10-12] to the graphical plots in the EPRI report and in Appendix A of Section XI of the ASME code [13]. Errors were found in the EPRI tabular data that were corrected, and an amended database was generated and reported in Ref. [6].

The EPRI database (consisting of 171 K_{Ic} data points) includes data from 11 materials using compact tension C(T) and wedge-open-loading (WOL) test specimens ranging in size from 1T to 11T as summarized in Table 1. All 171 K_{Ic} data points are plotted in Fig. 1 as a function of test temperature. The same data in Fig. 1 are replotted in Fig. 2 with the test temperature being normalized by the reference nil-ductility transition temperature, RT_{NDT}. The ASME K_{Ic} curve (from Figure A-4200-1 of Ref. [13]) is plotted in Fig. 2 as a solid line; the dashed line in Fig. 2 is an extension of the ASME K_{Ic} curve using the equation given in Ref. [13].

At ORNL, a survey was conducted to identify available K_{Ic} data generated more recently from pressure vessel steels that could augment the amended EPRI database published by Nanstad et al [6]. That survey produced an additional 83 K_{Ic} fracture toughness values (obtained from Refs. 14-18) that are plotted in Fig. 3 as a function of normalized temperature ($T - RT_{NDT}$). These new data came from seven materials, including HSSI Weld 72W, HSSI Weld 73W, HSST Plate 13A, A508 Class 3, Midland Nozzle Course Weld, Midland Beltline, and HSSI Plate 02 4th Irradiation Series. The tests used predominantly compact tension specimens ranging in size from C(T)-1T to C(T)-4T. The extended K_{Ic} database, compiled from the amended EPRI data and from the ORNL survey, provided a total of 254 fracture toughness data points for input to the statistical model development described in Ref. [1] and applied herein. A plot of the extended K_{Ic} database versus ($T - RT_{NDT}$) is given in Fig. 4; the complete tabulation of the database is included in Ref. [1]. Table 1 provides additional details concerning the extended dataset, and the chemistry and heat treatment of the principal materials in the dataset are given in Table 2.

2.2 K_{Ia} Database

The ORNL survey of available K_{Ia} data produced an additional 62 fracture toughness values [19-21] that were used to augment the 50 K_{Ia} data points [22, 23] obtained from the EPRI report [5]. Sources and summary details of the additional data are identified in Table 3. A plot of the original EPRI dataset is given in Fig. 5; the additional K_{Ia} data are plotted in Fig. 6; and the combined dataset is presented in Fig. 7. The extended database consisting of 112 fracture toughness values provided the input to the statistical model development for K_{Ia} described in Ref. [1]. A complete tabulation of the K_{Ia} database is included in Ref. [1].

3. Description Of New ORNL Statistical Models

In Ref. [1], new statistical representations for K_{Ic} and K_{Ia} were constructed from the extended fracture toughness databases described in Section 2. A two-parameter Weibull distribution, with the parameters calculated by the *Method of Moments* point-estimation technique, forms the basis for the new statistical models for which the test temperature is normalized by the reference-nil-ductility-transition temperature, RT_{NDT}. Those models are summarized below in both graphical and equation form.

3.1 Background

A previous study [24] investigated the EPRI K_{Ic} database in the context of the *Master Curve* [25-28] where the test temperature is normalized by the reference temperature, T_0, and size corrections are applied to the toughness data to allow the comparison of data from a range of specimen sizes. A Weibull distribution is assumed in Ref. [27] in which the shape parameter is fixed at 4 and the location parameter is fixed at the experimentally-determined value of 18.2 ksi-√in. (20 MPa-√m). The shape parameter of 4 is derived [25] from a theoretical treatment of cleavage initiation in which "weakest-link" mechanisms are assumed to dominate the scatter in the data at a given test temperature. This assumption allows a relationship to be developed between the probability of failure by cleavage and the stress and strain fields ahead of the crack front as characterized by the applied stress-intensity factor K_I. When two parameters are fixed, the Weibull model becomes a 1-parameter Weibull distribution in which the density is described by

$$w(x \mid b) = \frac{4}{b} y^3 \exp(-y^4) \;\; (y = (x - 18.2)/b, x > 18.2; b > 0)$$

where, in Ref. [27], $b = (K_0 - K_{\min})$ and $K_{\min}$ = 18.2 ksi-√in. (20 MPa-√m). With the 1-parameter Weibull distribution, the scale parameter, b or specifically K_0, is estimated in Ref. [27] with a maximum likelihood point estimator.

Due to the heterogeneity of the K_{Ic} database with its range of materials and specimen sizes (in some cases within the same grouping of replicate tests when normalized by RT_{NDT}), it was not clear that the theoretical treatment developed in previous studies necessarily accounted for all of the dominant modes that produced the observed scatter in the data. Figure 8 presents the EPRI database plotted as function of temperature normalized by RT_{NDT} (Fig. 8a) and by the T_0 [27] reference temperatures (Fig. 8b) calculated for this database [24]. A comparison of Figs. 8a and 8b indicates that the use of RT_{NDT} as a normalizing index results in a data scatter component that is not evident when T_0 is applied. Therefore, the decision was taken in Ref. [1] to develop a strictly statistical model to characterize the trends and scatter in the extended K_{Ic} database and, subsequently, in the K_{Ia} database.

3.2 The K_{Ic} Model

In the case of the Weibull distribution, there are three parameters to estimate, and these refer to the location, a, of the random variate, the scale, b, of the random variate, and most importantly, the shape parameter, c. The density is given by

$$w(x|a,b,c) = \frac{c}{b} y^{c-1} \exp\left(-y^c\right), \;\; (y = (x-a)/b, x > a,\, b,c > 0) \tag{1}$$

The Weibull density is derived from its cumulative distribution function

$$\Pr(X < x) = 1 - \exp(-y^c), \;\; (y = (x-a)/b, x > a,\, b,c > 0) \tag{2}$$

The K_{Ic} density, $w(x|\, a_2{**}(\Delta T), b_2{**}(\Delta T))$, is given as follows [1]:

$$w(x \mid a_2^{**}(\Delta T)\;, b_2^{**}(\Delta T)\;) = \frac{c(\Delta T)}{b_2^{**}(\Delta T)} y^{c(\Delta T)-1} \exp(-y^{c(\Delta T)}), \quad (y = (x - a_2^{**}(\Delta T)\;)/b_2^{**}(\Delta T)\;) \tag{3}$$

where the parameters of the distribution are given by [1]

$$\boxed{\begin{aligned} a_2^{**}(\Delta T) &= 10.8957 + 23.4192\exp(0.0023(\Delta T)) \ \ [\text{ksi}-\sqrt{\text{in.}}] \\ b_2^{**}(\Delta T) &= 14.7582 + 42.6312\exp(0.0124(\Delta T)) \ \ [\text{ksi}-\sqrt{\text{in.}}] \\ c(\Delta T) &= 2.03025 + 0.4983\exp(0.0135(\Delta T)) \end{aligned}} \tag{4}$$

with $x = K_{Ic}$ in ksi-√in., $\Delta T = (T\text{-}RT_{NDT})$ is in °F.

Figure 9 (from Ref. [1]) shows a plot of the lower boundary curve, a_2**, and the 1, 50, 95, 99, and 99.5 percentile curves, along with the extended K_{Ic} database.

3.3 The K_{Ia} Model

The K_{Ia} density, $w(x|\, a_2^{**}(\Delta T), b_2^{**}(\Delta T))$, is given as follows [1]:

$$w(x \mid a_2^{**}(\Delta T)\ , b_2^{**}(\Delta T)\ ) = \frac{2.5}{b_2^{**}(\Delta T)}\, y^{1.5}\exp(-y^{2.5}), \qquad (y = (x - a_2^{**}(\Delta T)\ )\,/\, b_2^{**}(\Delta T)\ ) \tag{5}$$

where the parameters of the distribution are given by [1]

$$\boxed{\begin{aligned} a_2^{**}(\Delta T) &= 24.584 + 15.352\exp(0.012639(\Delta T)) \ \ [\text{ksi}\sqrt{\text{in.}}] \\ b_2^{**}(\Delta T) &= 36.201 + 0.060307\,(\Delta T) \ \ [\text{ksi}\sqrt{\text{in.}}] \\ c &= 2.5 \end{aligned}} \tag{6}$$

with $x = K_{Ia}$ in ksi√in., $\Delta T = (T\text{-}RT_{NDT})$ is in °F.

Figure 10 (from Ref. [1]) shows a plot of the lower boundary curve, a_2**, and the 1, 50, 95, 99, and 99.5 percentile curves, along with the extended K_{Ia} database.

3.4 Example Problem Applying the New Statistical Model for K_{Ic}

As an example of how to apply the new statistical model for K_{Ic}, let the test temperature be T = -5 °F for a material with RT_{NDT} = 5 °F; therefore, $\Delta T = T - RT_{NDT}$ = -10 °F. We then calculate the parameters of the model by Eq. (4), repeated in Eq. (7):

$$
\begin{aligned}
a_2^{**}(\Delta T) &= 10.8957 + 23.4192\exp(0.0023(\Delta T)) \ \ [\text{ksi}\sqrt{\text{in.}}] \\
b_2^{**}(\Delta T) &= 14.7582 + 42.6312\exp(0.0124(\Delta T)) \ \ [\text{ksi}\sqrt{\text{in.}}] \\
c(\Delta T) &= 2.03025 + 0.4983\exp(0.0135(\Delta T))
\end{aligned} \tag{7}
$$

$$
\boxed{
\begin{aligned}
a_2^{**}(-10) &= 10.8957 + 23.4192\exp(0.0023(-10)) = 33.78241 \ \ [\text{ksi}\sqrt{\text{in.}}] \\
b_2^{**}(-10) &= 14.7582 + 42.6312\exp(0.0124(-10)) = 52.41774 \ \ [\text{ksi}\sqrt{\text{in.}}] \\
c(-10) &= 2.03025 + 0.4983\exp(0.0135(-10)) = 2.46562
\end{aligned}
}
$$

Solving Eq. (2) for the fracture toughness, *x,* produces a relation that can be used to construct percentile curves as a function of ΔT:

$$
x_p(\Delta T) = \{-\ln(1-p)\}^{1/c(\Delta T)} b_2^{**}(\Delta T) \ + a_2^{**}(\Delta T). \qquad (0 < p < 1) \tag{8}
$$

where p is the probability of failure. The median value of K_{Ic} representing a 50 percent cumulative probability of failure is then $x_{0.5}$. From Eq. (8) with $p = 0.5$

$$
\boxed{x_{0.5}(-10) = \{-\ln(1-0.5)\}^{1/2.46562} 52.41774 + 33.78241 = 78.96 \ \ [\text{ksi}\sqrt{\text{in.}}]}
$$

For a 1 percent cumulative probability of failure, the corresponding value of K_{Ic} is $x_{0.01}$ calculated from Eq. (8) with $p = 0.01$

$$
\boxed{x_{0.01}(-10) = \{-\ln(1-0.01)\}^{1/2.46562} 52.41774 + 33.78241 = 41.90 \ \ [\text{ksi}\sqrt{\text{in.}}]}
$$

Additional properties of the distribution may also be calculated, for example the mean and standard deviation at this normalized temperature are

Mean:

$$
K_{Ic(mean)}(-10) = a_2^{**}(-10) \ + b_2^{**}(-10) \ \Gamma(1 + 1/c(-10)) = \boxed{80.28 \ [\text{ksi}\sqrt{\text{in.}}]}
$$

Standard Deviation:

$$
\sigma(-10) = b_2^{**}(-10)\sqrt{\{\Gamma(1+2/c(-10)) - \Gamma^2(1+1/c(-10))\}} = \boxed{20.14 \ [\text{ksi}\sqrt{\text{in.}}]}
$$

Note that for an asymmetric distribution, the median and the mean are not the same.

3.5 Comparison with the IPTS Model

Figures 11 and 12 present the new K_{Ic} and K_{Ia} statistical models, respectively, compared to the K_{Ic} and K_{Ia} IPTS models. The IPTS K_{Ic} model in FAVOR assumes that the ASME K_{Ic} curve is positioned at K_{mean} - 2σ where K_{mean} is the mean of a normal distribution with standard deviation, σ. The standard deviation is assumed to be equal to 0.15 K_{mean} for K_{Ic} and 0.10 K_{mean} for K_{Ia}. Therefore, for K_{Ic} the estimated IPTS $K_{Ic\text{-}mean} = K_{Ic\text{-}ASME} / 0.7$, and for K_{Ia} the estimated IPTS $K_{Ia\text{-}mean} = K_{Ia\text{-}ASME} / 0.8$. Using these assumptions, the percentile curves at 50 percent (mean = median of a normal distribution), 0.135 percent (median - 3σ), 2.275 percent (median - 2σ), 97.725 percent (median + 2σ), and 99.865 percent (median + 3σ) can be plotted for the IPTS model and compared to the corresponding percentiles based on the new Weibull model. Note that for an asymmetric distribution, the mean of a Weibull density is not equal to its median, where the median corresponds to the 50 percentile curve.

4. Applications To RPV Assessments

The new ORNL statistical representations of the expanded K_{Ic} and K_{Ia} databases [see Eqs. (3)-(6)] were implemented in a development version of the FAVOR fracture mechanics computer code [4, 29]. That new implementation was applied to probabilistic fracture mechanics (PFM) analyses of selected RPVs, and the results were compared with those generated from earlier applications of IPTS methodology to the same vessels. Those comparisons serve to quantify the relative influence of the ORNL statistical representations on computed initiation and failure probabilities for certain PTS scenarios.

The problem statement for the first application utilized the dominant transients for the Calvert Cliffs unit 1 RPV (transients 8.1, 8.2 and 8.3 in Ref. [2]) and the embrittlement map specified in the RVID database [30-31]. These transients are illustrated in Figs. 13a-13c. The specified flaw characterization was derived from inspection of the PVRUF vessel, consisting of embedded flaws exclusively [32]. Each of these flaws was determined to be a planar crack-like defect. The radiation-induced shift in RT_{NDT} was calculated using Regulatory Guide 1.99, Revision 2 [33].

Probabilistic assessment of the RPV required representations of both the cleavage initiation and arrest fracture toughness databases. The first application focused on evaluation of

the ORNL statistical model for K_{Ic} [Eqs. (3)-(4)] by comparing results from that model with those from the IPTS model (see Fig. 11). The IPTS representation for K_{Ia} (shown in Fig. 12) was employed exclusively in these comparative analyses, i. e., the ORNL statistical model for K_{Ia} was not used for this case. Figure 14 depicts the conditional probability of crack initiation, designated by $P(I|E)$, as a function of RPV operating time, EOL, computed for transients 8.2 and 8.3 using the ORNL and IPTS fracture toughness models. The parameter EOL corresponds to the neutron fluence map at *end-of-licensing* specified in the RVID database. In these analyses, it was assumed that neutron fluence increases linearly with the operating time of the RPV. For both transients, application of the ORNL statistical representation produced higher values of $P(I|E)$ relative to IPTS K_{Ic} methodology. In Fig. 15, application of the ORNL K_{Ic} methodology is shown to produce an increase in $P(I|E)$ (compared to IPTS results) for transients 8.1, 8.2, and 8.3 that varied from 15 to 50 percent over the RPV operating life.

Figure 16 is a scatter plot illustrating values of ($T\text{-}RT_{NDT}$, K_{Ic}) for which cleavage fracture initiations were predicted in PFM analyses of transient 8.2 at EOL. Application of the ORNL statistical representation for K_{Ic} is compared with that of the IPTS methodology. Figure 17 is a similar plot that compares PFM initiation results for transient 8.3. These plots imply that the ORNL K_{Ic} model predicts crack initiations over a wider range of normalized temperature ($T\text{-}RT_{NDT}$) when compared with the IPTS methodology.

In a second application, PFM analyses were performed using the parameters of Calvert Cliffs RPV analyses described above, but with a fracture toughness model that incorporated the ORNL statistical representations for both K_{Ic} and K_{Ia}. In Fig. 18, application of the ORNL statistical models to transient 8.2 predicts a reduction in $P(F|E)$ compared to that of the IPTS methodology. Even though the ORNL K_{Ic} model predicts more flaws to initiate in cleavage fracture, the new K_{Ia} methodology predicted a higher percentage of stable arrests for the initiated flaws. Consequently, a smaller number of initiated flaws propagate through the wall to fail the vessel when compared to the IPTS methodology. For transient 8.3, application of the ORNL methodology produced an increase in $P(F|E)$ relative to the IPTS methodology. A distinguishing characteristic of transient 8.3 is a severe late repressurization. There are few stable crack arrests for the latter case, regardless of the computational methodology used to simulate crack propagation through the RPV wall. Figure 19 illustrates that the ORNL K_{Ic} and K_{Ia} models

predicted an increase in $P(F|E)$ for transient 8.3 that ranged between 20 and 40 percent over the RPV operating life when compared to IPTS methodology. For transients 8.1 and 8.2, $P(F|E)$ decreased between 40 percent and 70 percent over the operating life.

In a third application, comparative PFM analyses were performed for the Oconee unit 1 RPV [3] utilizing three of the most dominant transients (designated as TBVG, MSLB, and LANL in Ref. [3]). It should be noted that all three of these transients have a late repressurization. The Oconee analyses employed the RPV embrittlement map from the RVID database [31] and flaw characterization from the PVRUF inspection [32]. Application of the ORNL K_{Ic} (but not K_{Ia}) model predicted an increase in $P(I|E)$ that varied from 50 to 500 percent for the three transients over the operating life of the RPV (see Fig. 20). An increase in $P(F|E)$ as high as 300 percent is predicted when both the ORNL K_{Ic} and K_{Ia} representations are included in the fracture toughness model (Fig. 21).

5. Summary and Conclusions

- Comparisons of P(F|E) versus EOL curves generated from the ORNL and the IPTS representations of K_{Ic} and K_{Ia} revealed greater differences for the Oconee plant when compared with those for Calvert Cliffs. All three of the Oconee transients have a late repressurization.

- For the vessels and transients analyzed herein, application of the ORNL representation for K_{Ic} resulted in an increase of $P(I|E)$ when compared with IPTS methodology. Also, the ORNL K_{Ic} model predicted crack initiations over a wider range of normalized temperature ($T\text{-}RT_{NDT}$).

- Differences between predicted $P(F|E)$ versus EOL curves obtained from the ORNL and the IPTS representations of K_{Ic} and K_{Ia} appear to depend (at a minimum) on the PTS transient and the RPV embrittlement map. Of course, the overall $P(F|E)$ depends on variables in addition to those considered herein. Those variables include characterization of the flaw density, embedded versus surface-breaking flaw distributions, and effects of cladding. Thus, from the studies presented here, one cannot draw general conclusions about the overall $P(F|E)$ calculations based on an updated model of the fracture toughness transition in comparison with those of IPTS.

References

1. K. O. Bowman and P. T. Williams, *Technical Basis for Statistical Models of Extended K_{Ic} and K_{Ia} Fracture Toughness Databases for RPV Steels*, ORNL/NRC/LTR-99/27, Oak Ridge National Laboratory, February 2000.

2. D. L. Selby et al., Oak Ridge National Laboratory, *Pressurized-Thermal-Shock Evaluation of the Calvert Cliffs Unit 1 Nuclear Power Plant,* NUREG/CR-4022 (ORNL/TM-9408), September 1985.

3. T. J. Burns et al., Oak Ridge National Laboratory, *Preliminary Development of an Integrated Approach to the Evaluation of Pressurized- Thermal-Shock as Applied to the Oconee Unit 1 Nuclear Power Plant,* NUREG/CR-3770 (ORNL/TM-9176), May 1986.

4. T. L. Dickson, *FAVOR: A Fracture Analysis Code for Nuclear Reactor Pressure Vessels, Release 9401*, ORNL/NRC/LTR 94-1, Oak Ridge National Laboratory, February, 1994.

5. EPRI Special Report, 1978, *Flaw Evaluation Procedures: ASME Section XI*, EPRI NP-719-SR, Electric Power Research Institute, Palo Alto, CA.

6. R. K. Nanstad, J. A. Keeney, and D. E. McCabe, *Preliminary Review of the Bases for the K_{Ic} Curve in the ASME Code*, ORNL/NRC/LTR-93/15, Oak Ridge National Laboratory, Oak Ridge, TN, 1993.

7. *Standard Test Method for Plane-Strain Fracture Toughness of Metallic Materials,* E 399-90, Annual Book of ASTM Standards - Section 3: Metals Test Methods and Analytical Procedures, Vol. 03.01 Metals – Mechanical Testing; Elevated and Low-Temperature Tests; Metallography, American Society for Testing and Materials, West Conshohocken, PA, 1998.

8. ASME Boiler and Pressure Vessel Code, Section III, Article NB-2331, American Society of Mechanical Engineers, New York, NY, (1998).

9. *Standard Test Method for Determining Plane-Strain Crack-Arrest Fracture Toughness, K_{Ia}, of Ferritic Steels,* E 1221-88, Annual Book of ASTM Standards Section 3: Metals Test Methods and Analytical Procedures, Vol. 03.01 Metals – Mechanical Testing; Elevated and Low-Temperature Tests; Metallography, American Society for Testing and Materials, West Conshohocken, PA, 1998.

10. W. O. Shabbits, W. H. Pryle, and E. T. Wessel, *Heavy Section Fracture Toughness Properties of A533, Grade B, Class-1 Steel Plate and Submerged Arc Weldments*, HSST Technical Report 6, WCAP-7414, December 1969.

11. T. R. Mager, F. O. Thomas, and W. S. Hazelton, *Evaluation by Linear Elastic Fracture Mechanics of Radiation Damage to Pressure Vessel Steels,* HSST Technical Report 5, WCAP-7328, Revised, October 1969.

12. T. R. Mager, *Fracture Toughness Characterization Study of A533, Grade B, Class-1 Steel,* HSST Technical Report 10, WCAP-7578, October 1970.

13. ASME Boiler and Pressure Vessel Code, Section XI, Article A-4000: Material Properties, American Society of Mechanical Engineers, New York, NY, (1998) 413-417.

14. R. K. Nanstad, F. M. Haggag, and D. E. McCabe, *Irradiation Effects on Fracture Toughness of Two High-Copper Submerged-Arc Welds, HSSI Series 5,* USNRC Report NUREG/CR-5913 (ORNL/TM-12156/V1 and V2) Vol. 1 and 2, Oak Ridge National Laboratory, Oak Ridge, TN, October 1992.

15. D. E. McCabe. *A Comparison of Weibull and β_{Ic} Analysis of Transition Range Fracture Toughness Data,* USNRC Report NUREG/CR-5788 (ORNL/TM-11959), Oak Ridge National Laboratory, Oak Ridge, TN, January 1992.

16. T. Iawadate, Y. Tanaka, S. Ono, and J. Watanabe, "An Analysis of Elastic-Plastic Fracture Toughness Behavior for J_{Ic} Measurements in the Transition Region," *Elastic-Plastic Fracture: Second Symposium, Vol. II-Fracture Resistance Curves and Engineering Applications*, (edited by C. F. Shih and J. P. Gudas) ASTM STP 803, (1983) II531-II561.

17. D. E. McCabe, R. K. Nanstad, S. K. Iskander, and R. L. Swain, *Unirradiated Material Properties of Midland Weld WF-70,* USNRC Report NUREG/CR-6249 (ORNL/TM-12777), Oak Ridge National Laboratory, Oak Ridge, TN, October 1994.

18. J. J. McGowan, R. K. Nanstad, and K. R. Thoms, *Characterization of Irradiated Current-Practice Welds and A533 Grade B Class 1 Plate for Nuclear Pressure Vessel Service*, USNRC Report NUREG/CR-4880 (ORNL-6484/V1 and V2), Oak Ridge National Laboratory, Oak Ridge, TN, July 1988.

19. S. K. Iskander, W. R. Corwin, and R. K. Nanstad, *Results of Crack-Arrest Tests on Two Irradiated High-Copper Welds,* USNRC Report NUREG/CR-5584 (ORNL/TM-11575), Oak Ridge National Laboratory, Oak Ridge, TN, December 1990.

20. S. K. Iskander, C. A. Baldwin, D. W. Heatherly, D. E. McCabe, I. Remec, and R. L. Swain, *Detailed Results of Testing Unirradiated and Irradiated Crack-Arrest Toughness Specimens from the Low Upper-Shelf Energy, High Copper Weld, WF-70*, NUREG/CR-6621 (ORNL/TM-13764) under preparation.

21. S. K. Iskander, R. K. Nanstad, D. E. McCabe, and R. L. Swain, "Effects of Irradiation on Crack-Arrest Toughness of a Low Upper-Shelf Energy, High-Copper Weld," *Effects of Radiation on Materials: 19th International Symposium, ASTM STP 1366*, M. L. Hamilton, A. S. Kumar, S. T. Rosinski, and M. L. Grossbeck, 2000, pp. 245-265.

22. E. J. Ripling and P. B. Crosley, "Strain Rate and Crack Arrest Studies," *HSST 5th Annual Information Meeting*, Paper No. 9, 1971.

23. E. J. Ripling and P. B. Crosley, "Crack Arrest Studies," *HSST 6th Annual Information Meeting*, Paper No. 10, 1972.

24. M. A. Sokolov, "Statistical Analysis of the ASME K_{Ic} Database," *Transactions of the ASME* **120**, (1998) 24-28.

25. K. Wallin, "The Scatter in K_{Ic}-Results, *Eng. Fracture Mech.* **19**(6), (1984) 1085-1093.

26. J. G. Merkle, K. Wallin, and D. E. McCabe, *Technical Basis for an ASTM Standard on Determining the Reference Temperature, T_0, for Ferritic Steels in the Transition Range*, NUREG/CR-5504 (ORNL/TM-13631) Oak Ridge National Laboratory, November 1998.

27. "Standard Test Method for Determination of Reference Temperature, T_0, for Ferritic Steels in the Transition Range," E 1921-97, Annual Book of ASTM Standards Section 3: Metals Test Methods and Analytical Procedures, Vol. 03.01 *Metals – Mechanical Testing; Elevated and Low-Temperature Tests; Metallography*, American Society for Testing and Materials, West Conshohocken, PA, 1998.

28. M. Kirk and B. Hardies, "*Applications of Master Curve Technology*," (to be published) 2000.

29. T. L. Dickson, "An Overview of FAVOR: A Fracture Analysis Code for Nuclear Reactor Pressure Vessels," *Transactions of the 13th International Conference on Structural Mechanics in Reactor Technology (SMiRT 13),* Volume IV, pp 701-706, Porto Alegre, Brazil, August, 1995.

30. T. L. Dickson et al., "Revisiting the Integrated Pressurized Thermal Shock Studies of an Aging Pressurized Water Reactor," PVP-Volume 388, *Fracture, Design Analysis of Pressure Vessels, Heat Exchangers, Piping Components, and Fitness for Service*, ASME, August, 1999.

31. *Reactor Vessel Integrity Database*, NUREG-1511, U.S. Nuclear Regulatory Commission, December, 1994, NUREG-1511, Supplement 1, October, 1996; RVID Version 2.0, August, 1997.

32. G. J. Shuster, S. R. Doctor, and P. G. Heasler, Volume 1*, Characterization of Flaws in U.S. Reactor Pressure Vessels, Density and Distribution of Flaw Indications in PVRUF*, November, 1998, volume 3, *Density and Distribution of Flaw Indications in Shoreham Vessel*, NUREG/CR-6471, Pacific Northwest National Laboratory, November, 1999.

33. U. S. Nuclear Regulatory Commission, Regulatory Guide 1.99, Revision 2, *Radiation Embrittlement of Reactor Vessel Materials*, May 1988.

Table 1. Summary of K_{Ic} Extended Database

	Material	Source	Specimen Type	Size Range	Temp. Range (°F)	(T-RT_{NDT}) Range (°F)	No. of Data Points
EPRI	Database	EPRI NP-719-SR					
1	HSST 01 subarc weldment	Shabbits (1969)	C(T)	1T - 6T	-200 to -50	-200 to -50	8
2	A533B Cl. 1 subarc weld	Shabbits (1969)	C(T)	1T - 8T	-200 to 0	-200 to 0	8
3	HSST 01	Mager (1970)	C(T)	1T	-150	-170	17
4	HSST 03	Mager (1970)	C(T)	1T	-150	-170	9
5	A533B Cl. 1	Mager (1969)	WOL	1T - 2T	-320 to -150	-385 to -215	13
6	HSST 02	Mager (1969)	WOL & C(T)	1T - 2T	-200 to 0	-200 to 0	41
6	HSST 02	Shabbits (1969)	C(T)	1T - 11T	-250 to 50	-250 to 50	28
7	A533B Cl. 1 weldment	Mager (1969)	WOL	1T - 2T	-320 to -200	-275 to -155	10
8	A533 B Cl. 1 weldment/HAZ	Mager (1969)	WOL	1T - 2T	-320 to -200	-320 to -200	6
9	A508 Cl.2 European Forging	Mager (1969)	WOL	1T - 2T	-320 to -100	-370 to -150	12
10	A508 Class 2	unpublished	C(T)	2T - 6T	-150 to 0	-201 to -51	9
11	A508 Class 2	unpublished	C(T)	2T - 8T	-125 to -75	-190 to -30	10
						Total	171
Additional Data	Additional Data						
12	HSSI Weld 72W	NUREG/CR-5913.	C(T)	1T-4T	-238 to 5	-229 to 14	12
13	HSSI Weld 73W	NUREG/CR-5913	C(T)	1T-4T	-238 to -58	-209 to -29	10
14	HSST Plate 13A	NUREG/CR-5788	C(T)	1T-4T	-238 to -103	-229 to -94	43
15	A508 Cl. 3	ASTM STP 803	Bx2B C(T)	1T-4T	-238 to -4	-225 to 9	6
16	Midland Nozzle Course Weld	NUREG/CR-6249	C(T)	1T	-148 to -58	-200 to -110	6
17	Midland Beltline	NUREG/CR-6249	C(T)	1T	-148	-171	2
18	Plate 02 4th Irr. Series (68-71W)	NUREG/CR-4880	C(T)	1T	-148 to -139	-148 to -139	4
						Total	83
						Grand Total	254

References For Tables 1 And 2

EPRI Special Report, 1978, *Flaw Evaluation Procedures: ASME Section XI*, EPRI NP-719-SR, Electric Power Research Institute, Palo Alto, CA.

W. O. Shabbits, W. H. Pryle, and E. T. Wessel, Heavy Section Fracture Toughness Properties of A533, Grade B, Class-1 Steel Plate and Submerged Arc Weldments, HSST Technical Report 6, WCAP-7414, December 1969.

T. R. Mager, F. O. Thomas, and W. S. Hazelton, *Evaluation by Linear Elastic Fracture Mechanics of Radiation Damage to Pressure Vessel Steels,* HSST Technical Report 5, WCAP-7328, Revised, October 1969.

T. R. Mager, *Fracture Toughness Characterization Study of A533, Grade B, Class-1 Steel*, HSST Technical Report 10, WCAP-7578, October 1970.

R. K. Nanstad, F. M. Haggag, and D. E. McCabe, *Irradiation Effects on Fracture Toughness of Two High-Copper Submerged-Arc Welds, HSSI Series 5,* USNRC Report NUREG/CR-5913 (ORNL/TM-12156/V1 and V2) Vol. 1 and 2, Oak Ridge National Laboratory, Oak Ridge, TN, October 1992.

D. E. McCabe., *A Comparison of Weibull and β_{Ic} Analysis of Transition Range Fracture Toughness Data,* USNRC Report NUREG/CR-5788 (ORNL/TM-11959), Oak Ridge National Laboratory, Oak Ridge, TN, January 1992.

T. Iawadate, Y. Tanaka, S. Ono, and J. Watanabe, "An Analysis of Elastic-Plastic Fracture Toughness Behavior for J_{Ic} Measurements in the Transition Region," *Elastic-Plastic Fracture: Second Symposium, Vol. II-Fracture Resistance Curves and Engineering Applications*, ASTM STP 803, (1983) II531-II561.

D. E. McCabe, R. K. Nanstad, S. K. Iskander, R. L. Swain, *Unirradiated Material Properties of Midland Weld WF-70,* USNRC Report NUREG/CR-6249 (ORNL/TM-12777), Oak Ridge National Laboratory, Oak Ridge, TN, October 1994.

J. J. McGowan, R. K. Nanstad, and K. R. Thoms, *Characterization of Irradiated Current-Practice Welds and A533 Grade B Class 1 Plate for Nuclear Pressure Vessel Service*, USNRC Report NUREG/CR-4880 (ORNL-6484/V1 and V2), Oak Ridge National Laboratory, Oak Ridge, TN, July 1988.

Table 2. Chemistry and Heat Treatment of Principal Materials

Material ID	Specification	Source	Chemistry – wt (%)										Heat Treatment
			C	P	Mn	Ni	Mo	Si	Cr	Cu	S	Al	
HSST 01	A533B Cl. 1	Mager (1970)	.22	.012	1.48	.68	.52	.25	-	-	.018	-	Note 1
HSST 02	A533B Cl. 1	Mager (1969)	.22	.012	1.48	.68	.52	.25	-	-	.018	-	Note 2
HSST 03	A533B Cl. 1	Mager (1970)	.20	.011	1.26	.56	.45	.25	.10	.13	.018	.034	Note 3
HSST 02	A533B Cl. 1	Shabbits (1969)	.22	.012	1.48	.68	.52	.25	-	-	.018	-	Note 4
HSST 01 subarc weld	A533B Cl. 1	Shabbits (1969)	.12	.014	1.35	.65	.52	.23	-	-	.012	-	Note 5
B&W subarc weldment	A533B Cl. 1	Shabbits (1969)	.10	.009	1.77	.64	.42	.36	-	-	.015	-	Note 6
PW/PH weldment	A533B Cl. 1	Mager (1969)	.09	.019	1.25	1.08	.52	.23	.05	.22	.13	.037	Note 7
MD07 European	A508 Cl. 2 Ring forging	Mager (1969)	.18	.009	1.16	.72	.51	.24	.28	-	.10	-	Note 8
-	A533B Cl. 1	Mager (1969)	.19	.012	1.37	.52	.45	.25	.13	.15	.016	.048	Note 9
72W	A533B weld	5788	.09	.006	1.66	.60	.58	.04	.27	.23	.006	-	
73W	A533B weld	5788	.10	.005	1.56	.60	.58	.04	.25	.21	.005	-	

Notes:

1.	Normalizing:	1675 °F	4 hr, air cooled
	Austentizing:	1600 °F	4 hr
	Quenching:	Water quench	
	Tempering:	1225 °F	4 hr, furnace cooled
	Stress Relief:	1150 °F	40 hr, furnace cooled
2.	Normalizing:	1675 °F	4 hr, air cooled
	Austentizing:	1600 °F	4 hr
	Quenching:	Water quench	
	Tempering:	1225 °F	4 hr, furnace cooled
	Stress Relief:	1150 °F	40 hr, furnace cooled
3.	Normalizing:	1675 °F	12 hr, air cooled
	Austentizing:	1575 °F	12 hr
	Quenching:	Water quench	
	Tempering:	1175 °F	12 hr, furnace cooled
	Stress Relief:	1125 °F	40 hr, furnace cooled
4.	Normalizing:	1675 ± 25 °F	4 hr
	Austentizing:	1520 °F – 1620 °F	4 hr
	Quenching:	Water quench.	
	Tempering:	1200 °F – 1245 °F	4 hr, air cooled

	Stress Relief:	1150 ± 25 °F	40 hr, furnace cooled to 600 °F
5.	Post Weld:	1150 ± 25 °F	12 hr
	Intermediate	1100 ± 25 °F	15 min
6.	Post Weld	1100 °F – 1150 °F	12 hr
	Intermediate	1100 °F – 1150 °F	15 min
7.		620 °C	27 hr, air cooled
8.		925 °C	5 hr
	Quenching:	Water quench	
		650 °C	3 hr, furnace cooled
		620 °C	24 hr, air cooled
9.		910 °C	8 hr
	Quenching:	Water quench	
		680 °C	10 hr, furnace cooled
		850 °C	8 hr
	Quenching:	Water quench	
		690 °C	8 hr, air cooled
		620 °C	24 hr, air cooled

Table 3. Summary of K_{Ia} Extended Database

	Material	Source	Specimen Type	Size Range	Test Temp. Range (°F)	$(T\text{-}RT_{NDT})$ Range (°F)	No. of Data Points
EPRI	Database	EPRI NP-719-SR					
1	HSST 02	Ripling (1971)	C(T)	1T-3T	-150 to 121	-150 to 121	50
Additional Data	Additional Data						
2	HSSI Weld 72W	NUREG/CR-5584	C(T) crack arrest		-78 to 41	-68 to 51	32
3	HSSI Weld 73W	NUREG/CR-5584	C(T) crack arrest		-78 to 59	-48 to 89	26
4	MW15J	NUREG/CR-6621	C(T) crack arrest		-4 to 50	-36 to 18	4
						Total =	112

References For Table 3

EPRI Special Report, 1978, *Flaw Evaluation Procedures: ASME Section XI*, EPRI NP-719-SR, Electric Power Research Institute, Palo Alto, CA.

E. J. Ripling and P. B. Crosley, "Strain Rate and Crack Arrest Studies," *HSST 5th Annual Information Meeting*, Paper No. 9, 1971.

S. K. Iskander, W. R. Corwin, R. K. Nanstad, *Results of Crack-Arrest Tests on Two Irradiated High-Copper Welds,* USNRC Report NUREG/CR-5584 (ORNL/TM-11575), Oak Ridge National Laboratory, Oak Ridge, TN, December 1990.

S. K. Iskander, C. A. Baldwin, D. W. Heatherly, D. E. McCabe, I. Remec, and R. L. Swain, *Detailed Results of Testing Unirradiated and Irradiated Crack-Arrest Toughness Specimens from the Low Upper-Shelf Energy, High Copper Weld, WF-70,* NUREG/CR-6621 (ORNL/TM-13764) under preparation.

S. K. Iskander, R. K. Nanstad, D. E. McCabe, and R. L. Swain, "Effects of Irradiation on Crack-Arrest Toughness of a Low Upper-Shelf Energy, High-Copper Weld," *Effects of Radiation on Materials: 19th International Symposium, ASTM STP 1366*, M. L. Hamilton, A. S. Kumar, S. T. Rosinski, and M. L. Grossbeck, eds., American Society for Testing and Materials, to be published in 1999.

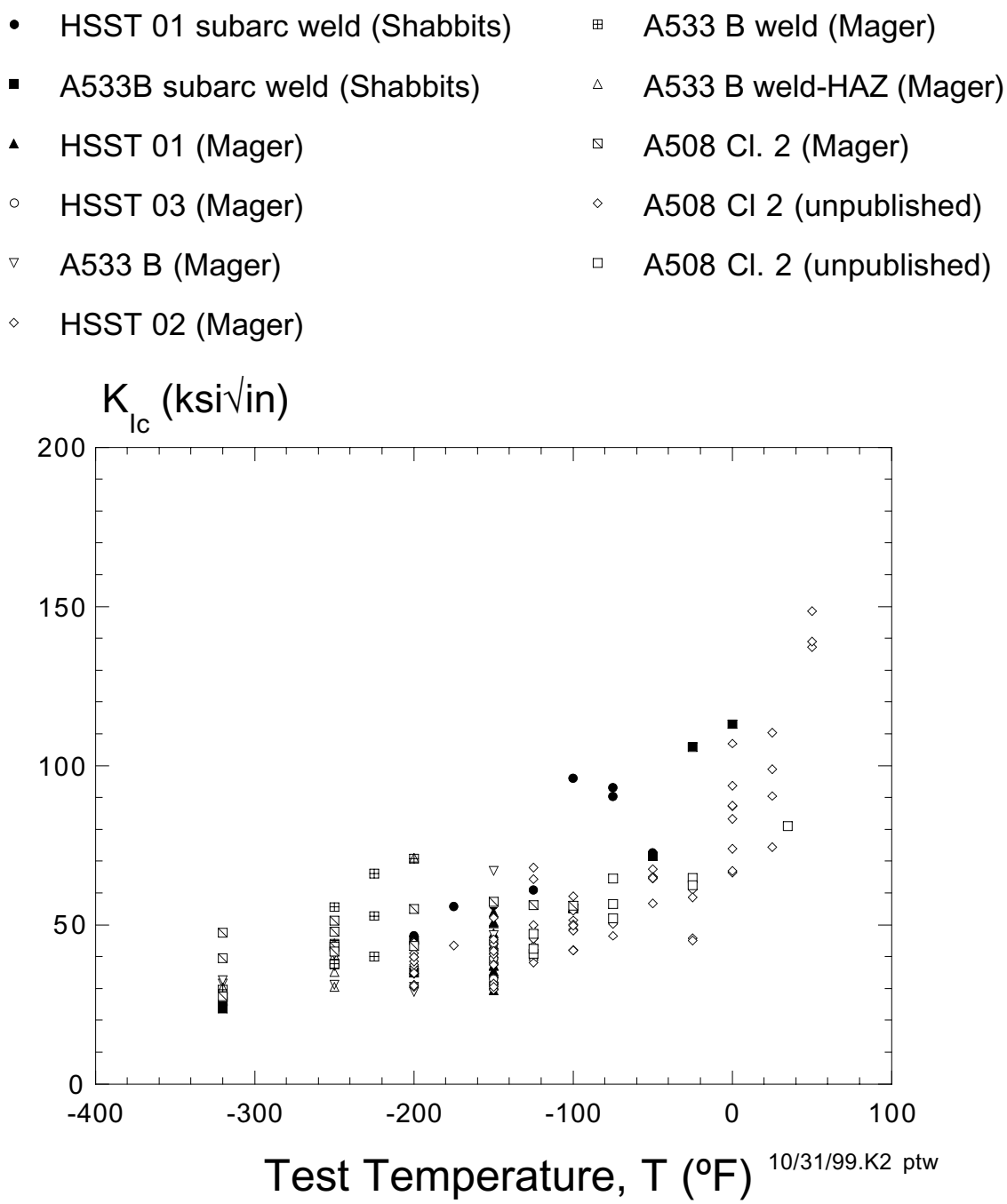

Fig. 1. Distribution of EPRI K_{Ic} database with test temperature.

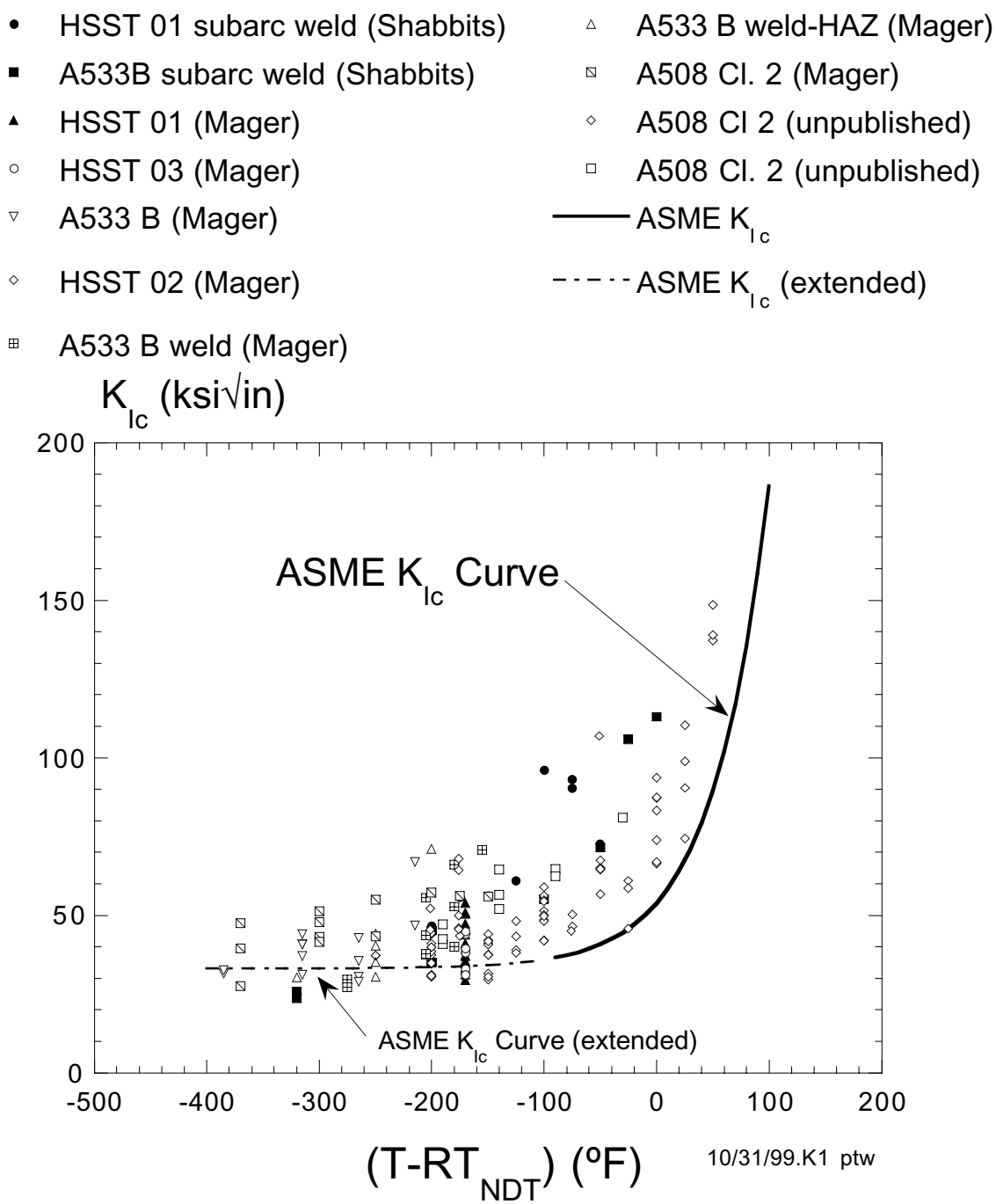

Fig. 2. Distribution of EPRI K_{Ic} database with normalized temperature (T - RT_{NDT}).

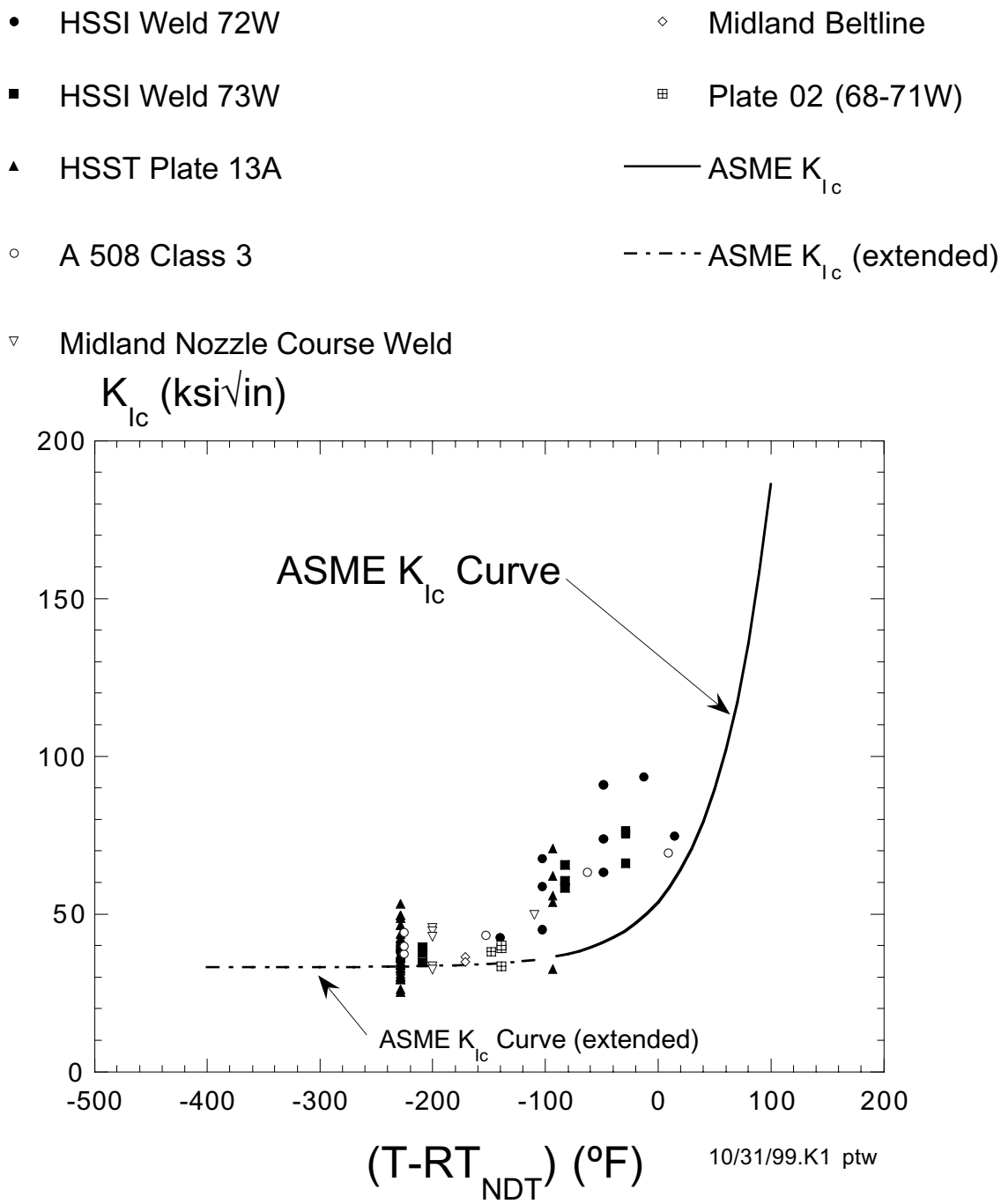

Fig. 3. Additional K_{Ic} data complied at ORNL.

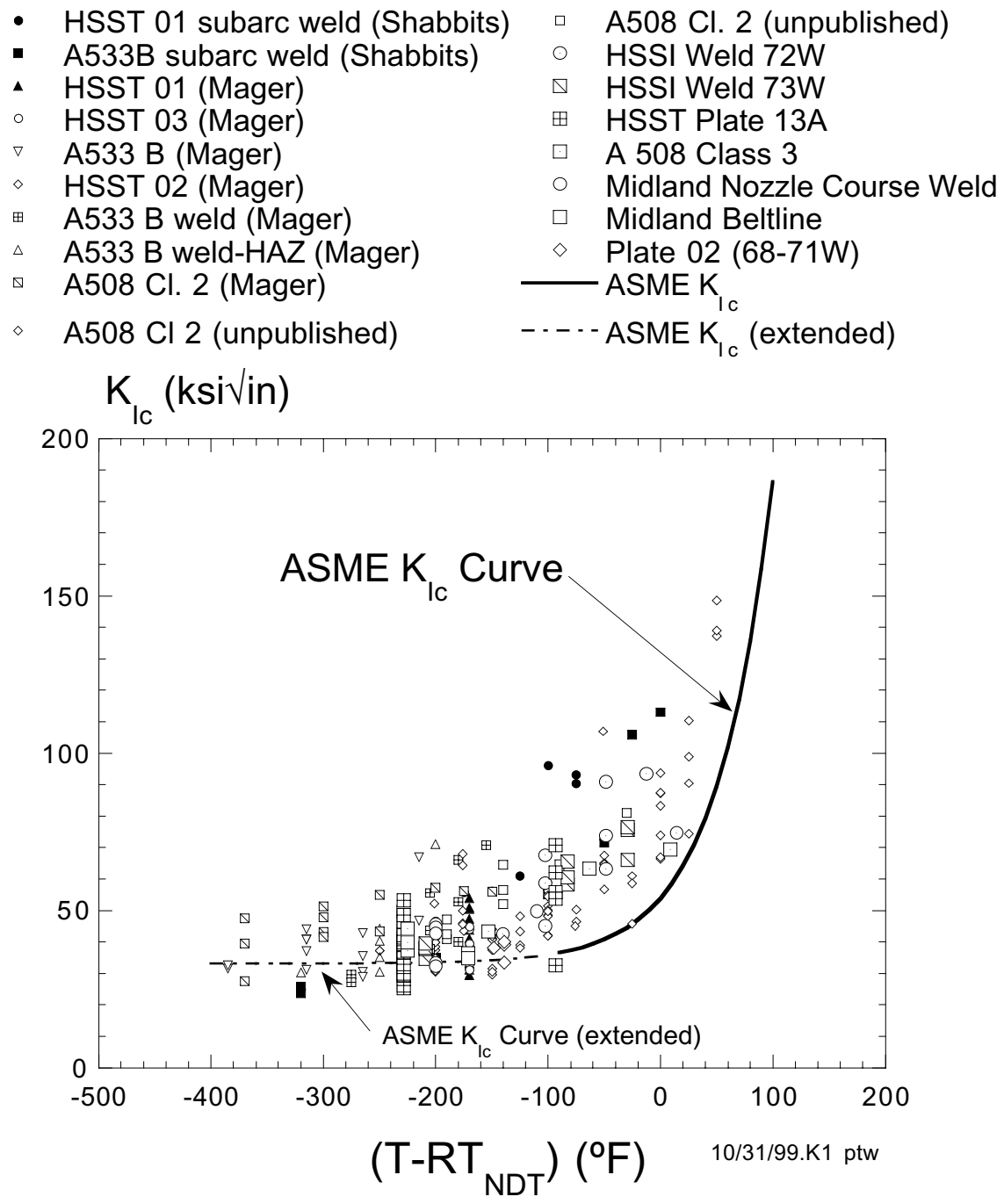

Fig. 4. Distribution of extended K_{Ic} database with normalized temperature ($T - RT_{NDT}$).

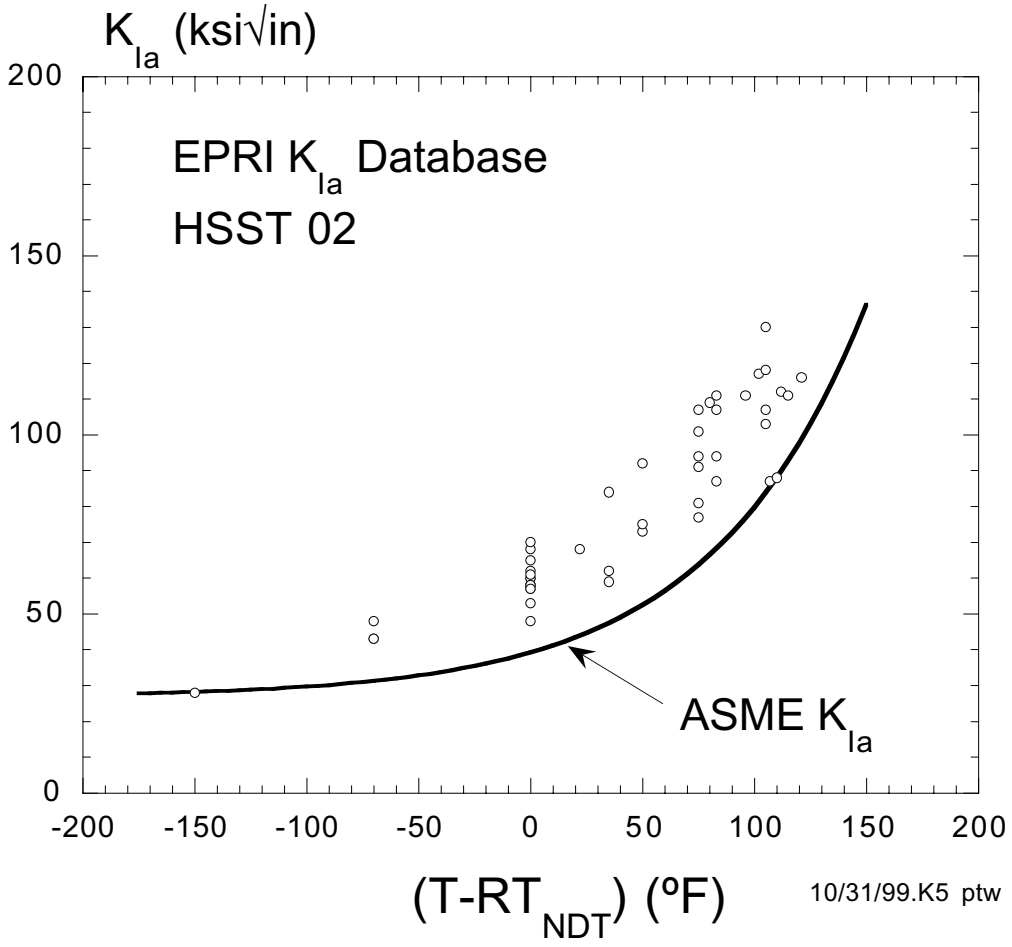

Fig. 5. Distribution of EPRI K_{Ia} database with normalized temperature ($T - RT_{NDT}$).

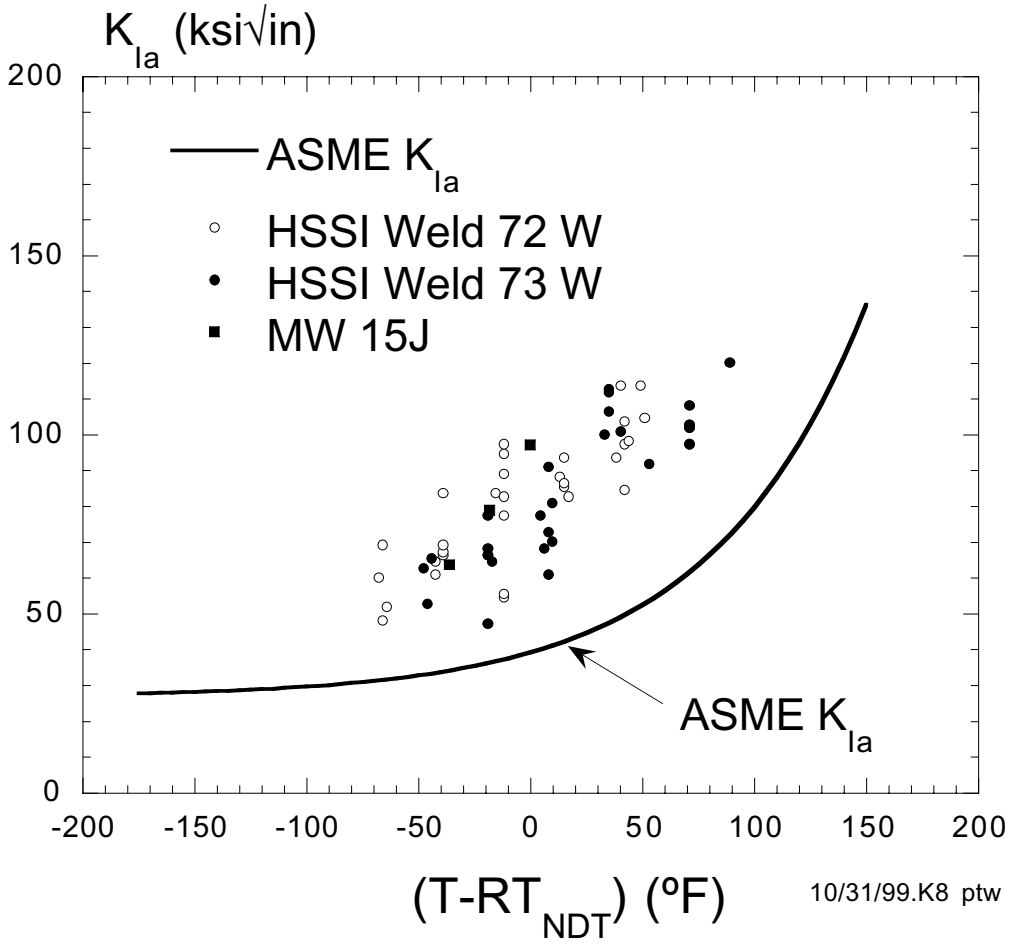

Fig. 6. Additional K_{Ia} data compiled at ORNL.

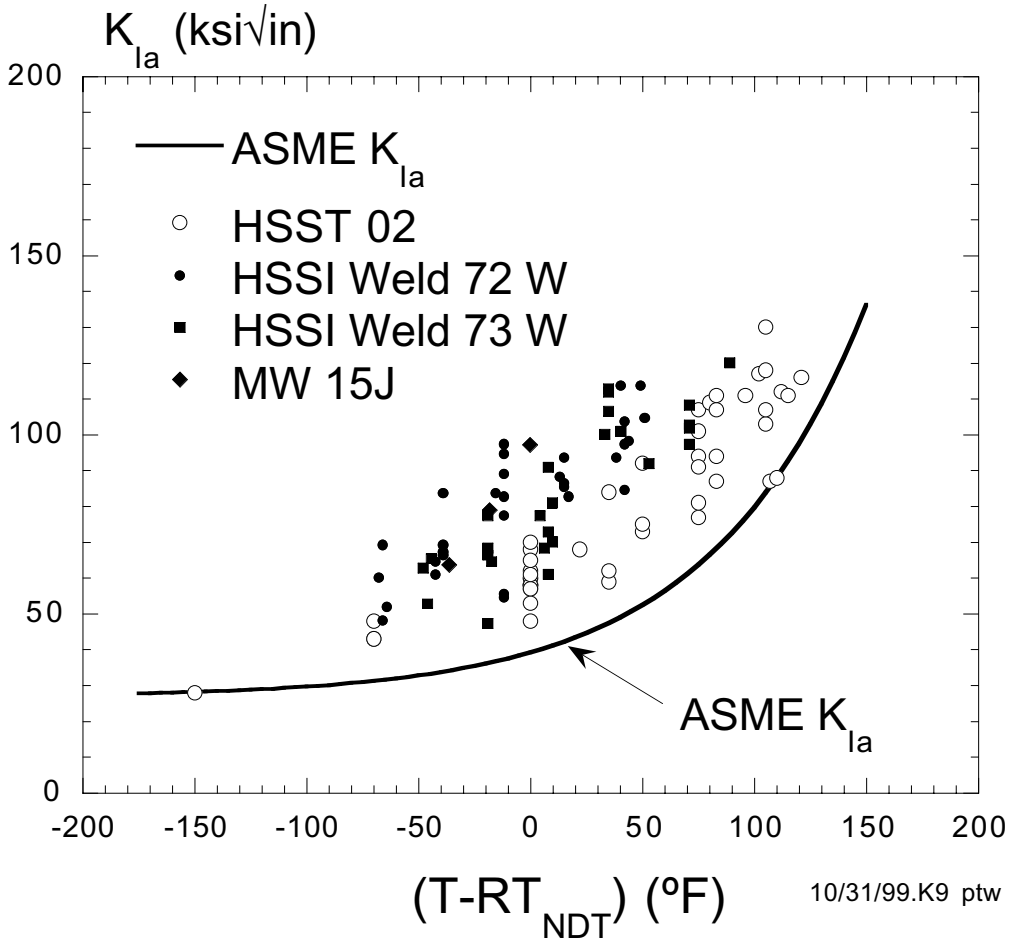

Fig. 7. Distribution of extended K_{Ia} database with normalized temperature ($T - RT_{NDT}$).

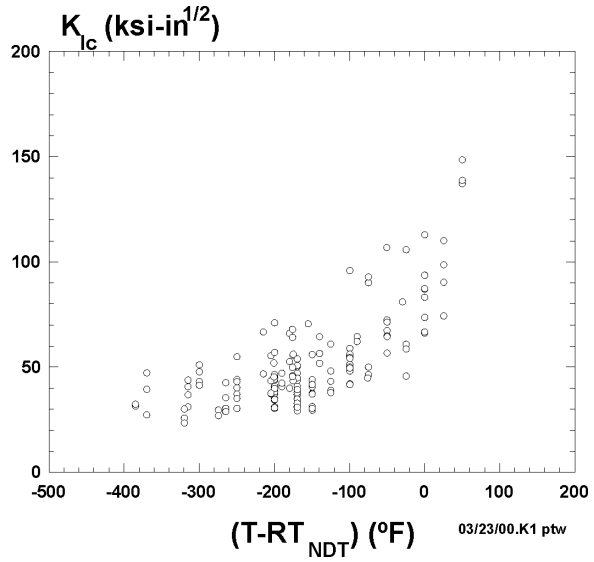

(a)

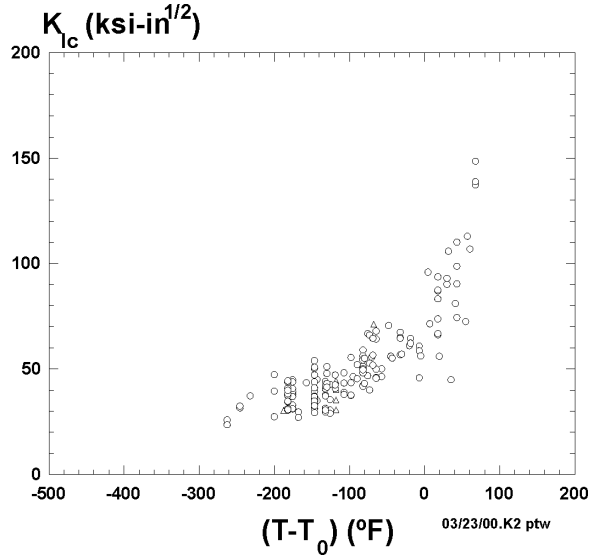

(b)

Fig. 8. Comparison of EPRI K_{Ic} database with test temperatures, T, normalized by (a) RT_{NDT} and (b) T_0.

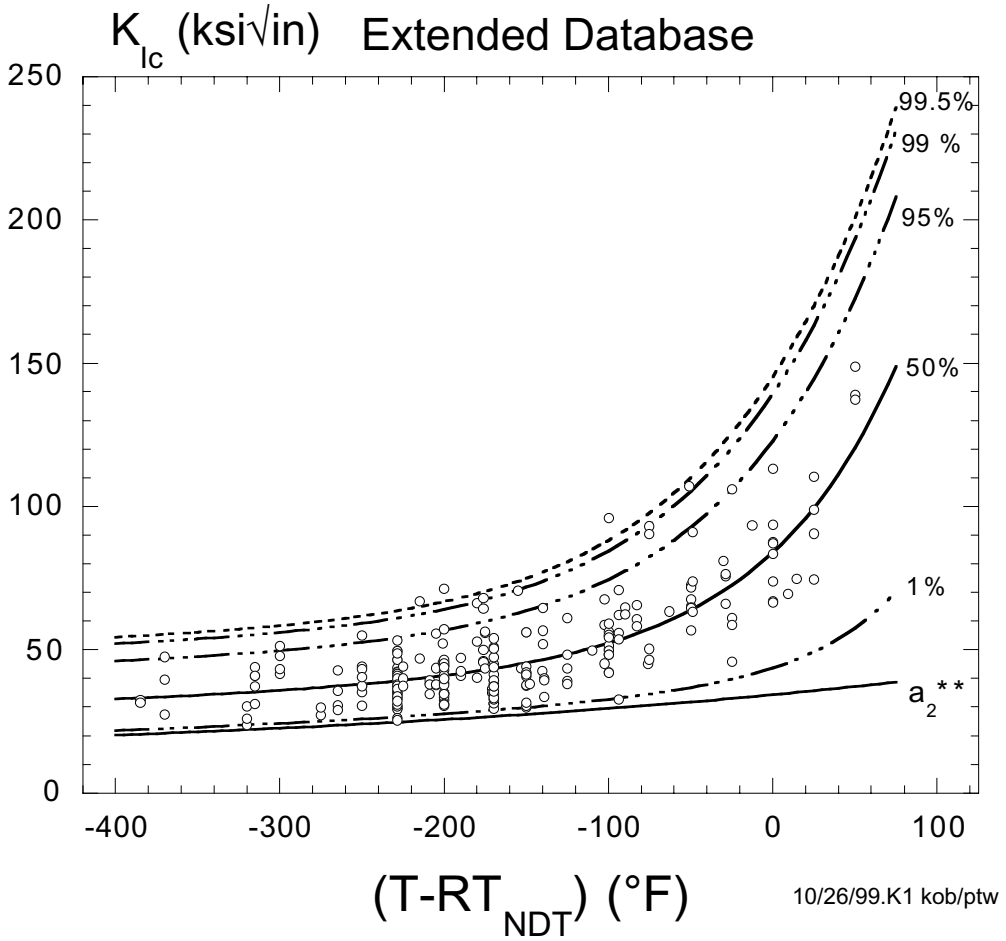

Fig. 9. Weibull model of K_{Ic} fracture toughness vs. normalized temperature (T - RT_{NDT}).

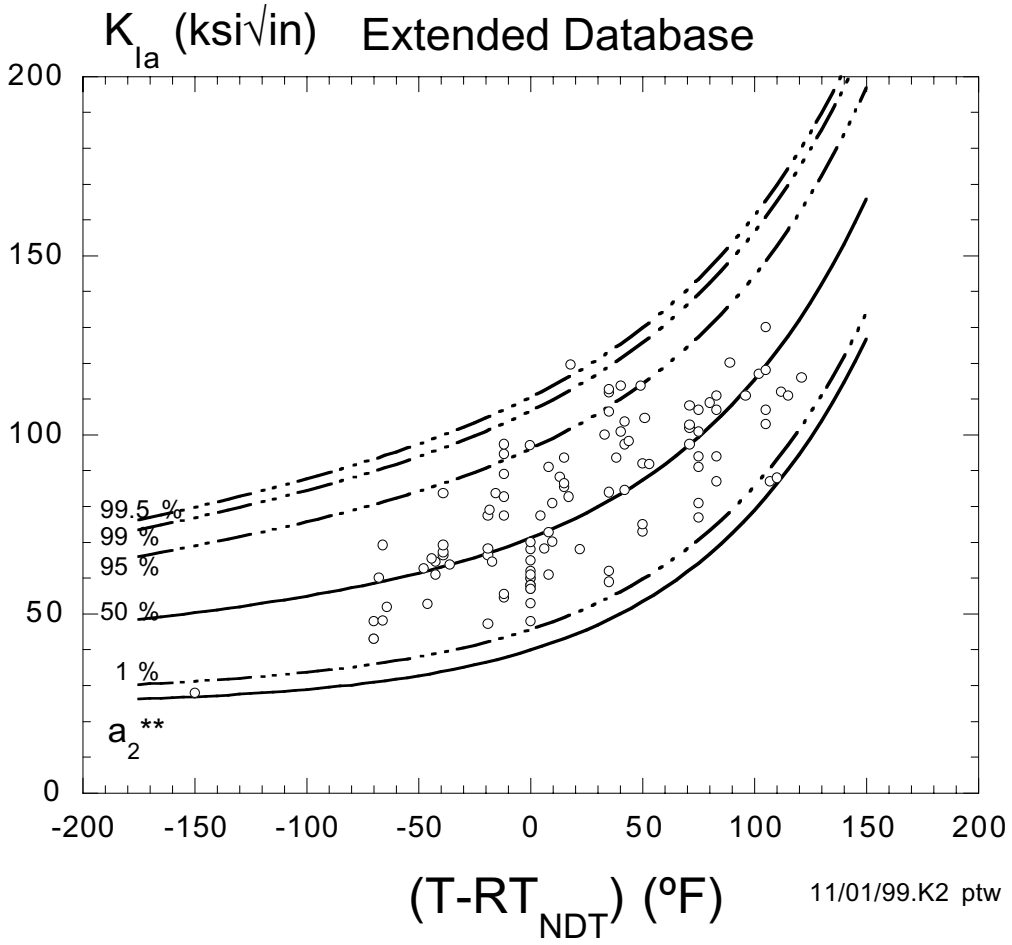

Fig. 10. Weibull model of K_{Ia} fracture toughness vs. normalized temperature (T - RT_{NDT}).

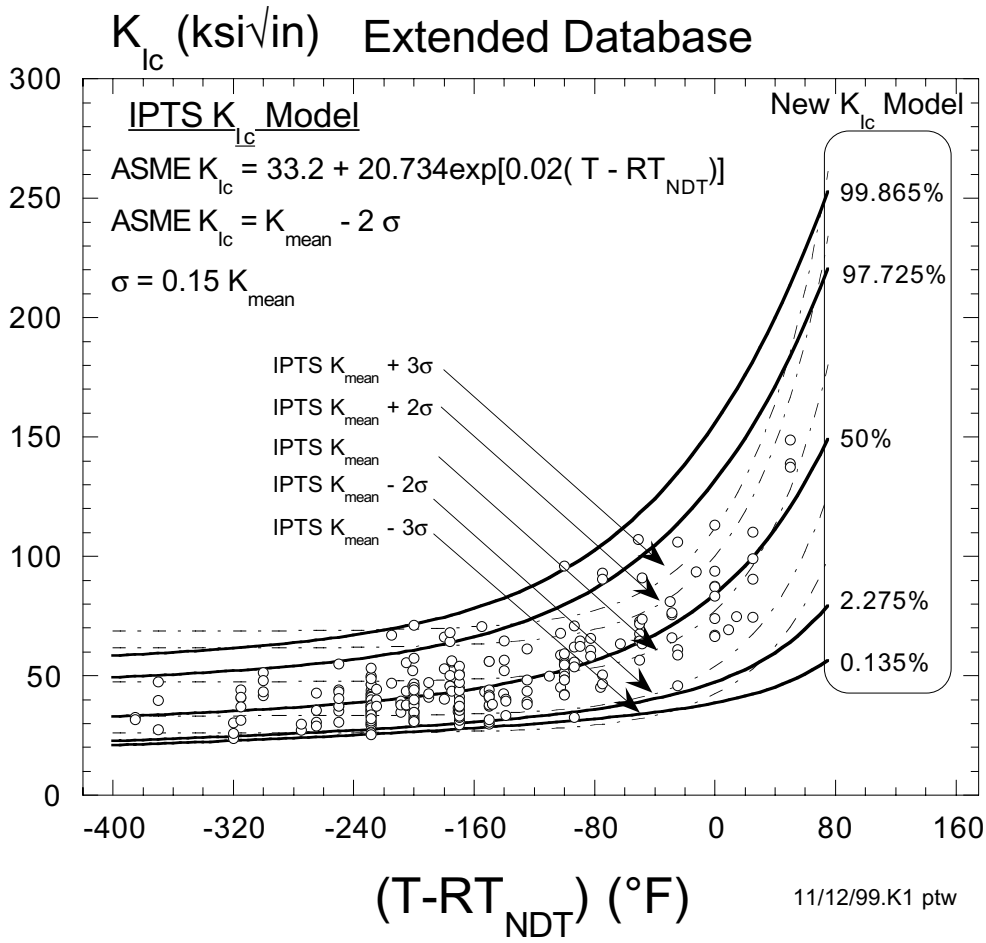

Fig. 11. New statistical model (solid curves) of the extended K_{Ic} database compared to the IPTS model (dashed curves) applied in FAVOR for Method 2 analyses.

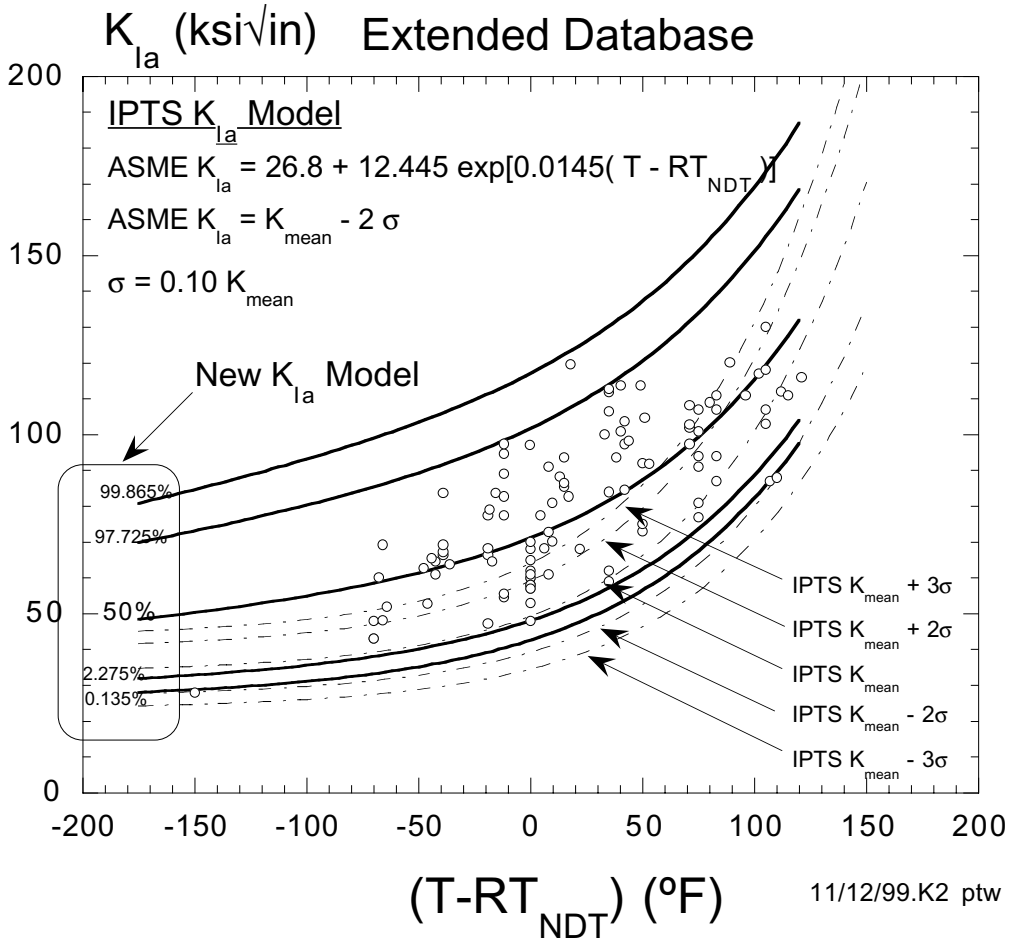

Fig. 12. New statistical model (solid curves) of the extended K_{Ia} database compared to the current IPTS model (dashed curves) applied in FAVOR for Method 2 analyses.

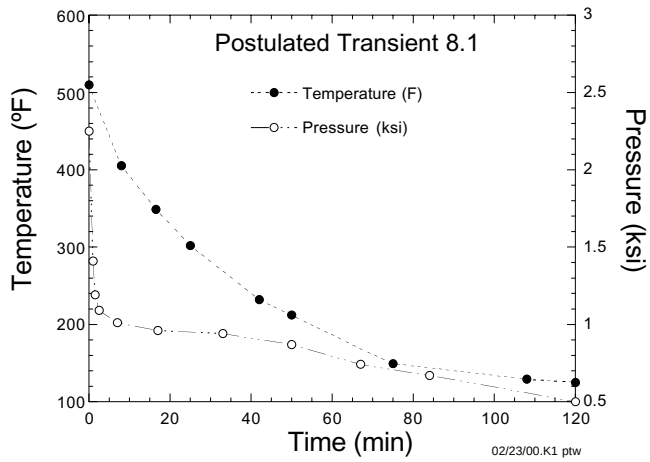

(a)

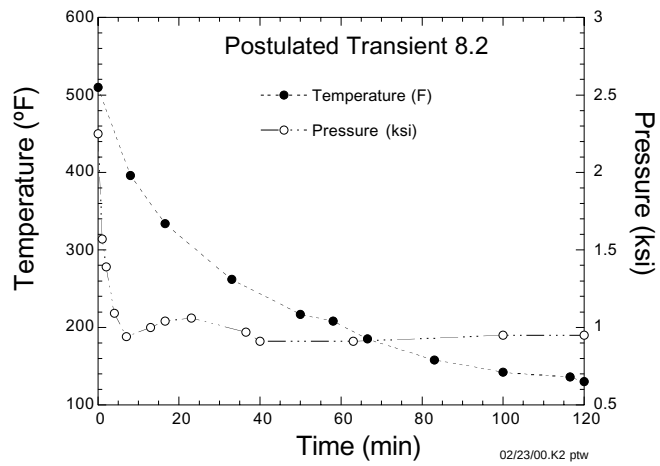

(b)

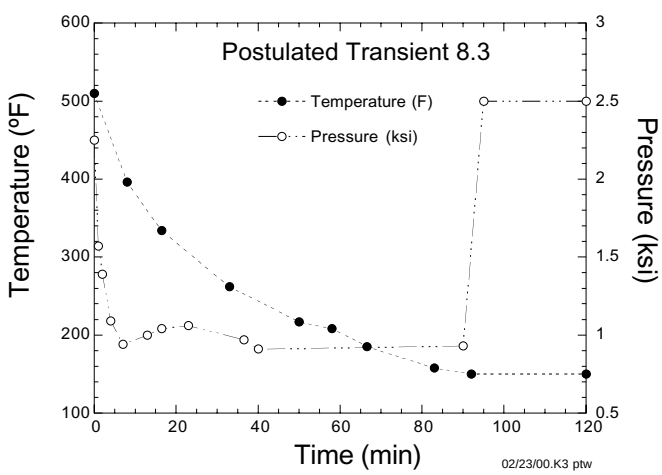

(c)

Fig. 13. Postulated transients (a) 8.1, (b) 8.2 and (c) 8.3.

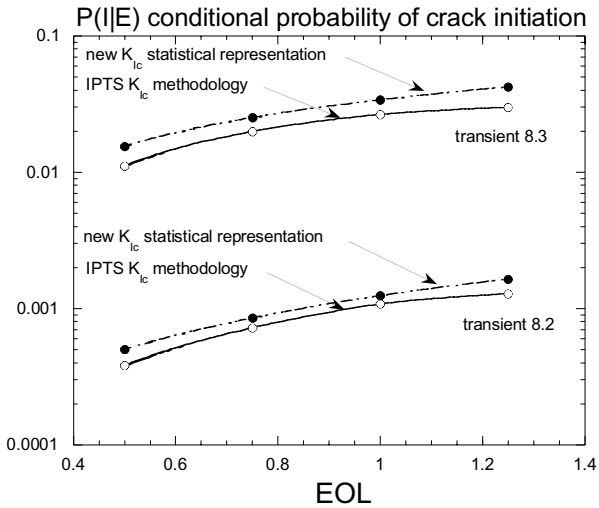

Fig. 14. Comparison of *P(I|E)* versus EOL from applications of the ORNL and IPTS K_{Ic} models to Calvert Cliffs dominant PTS transients 8.2 and 8.3.

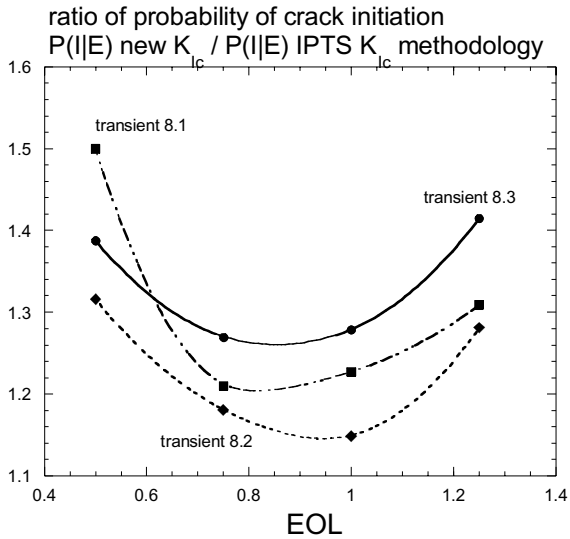

Fig. 15. Ratio of *P(I|E)*s computed in applications of the ORNL and IPTS K_{Ic} models to Calvert Cliffs dominant PTS transients 8.1, 8.2 and 8.3.

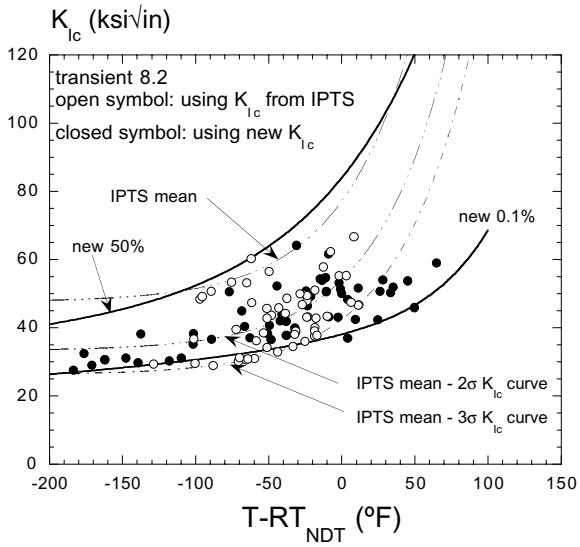

Fig. 16. Cleavage fracture initiations predicted at EOL for Calvert Cliffs transient 8.2.

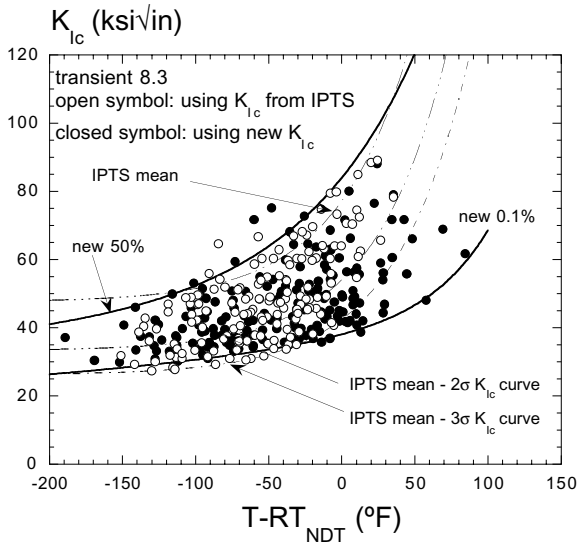

Fig. 17. Cleavage fracture initiations predicted at EOL for Calvert Cliffs transient 8.3.

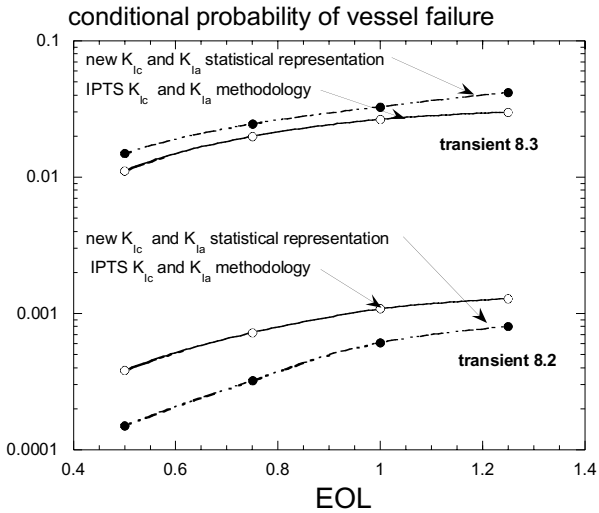

Fig 18. Comparison of *P(F|E)* versus EOL from applications of the ORNL and IPTS K_{Ic} and K_{Ia} models to Calvert Cliffs dominant PTS transients 8.2 and 8.3

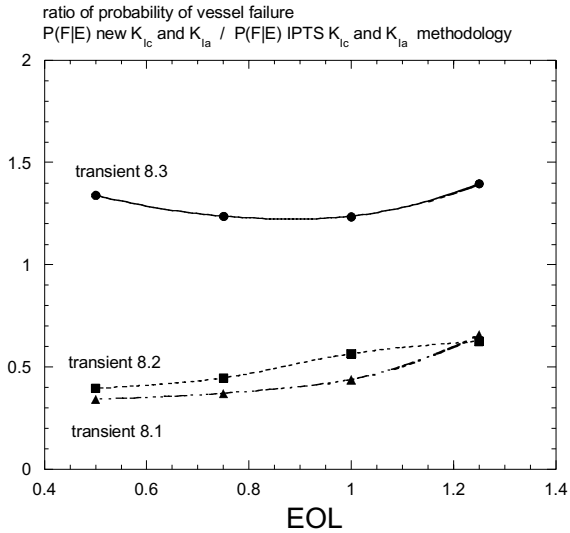

Fig. 19. Ratio of *P(F|E)*s computed in applications of the ORNL and IPTS K_{Ic} and K_{Ia} models to Calvert Cliffs dominant PTS transients 8.1, 8.2, and 8.3.

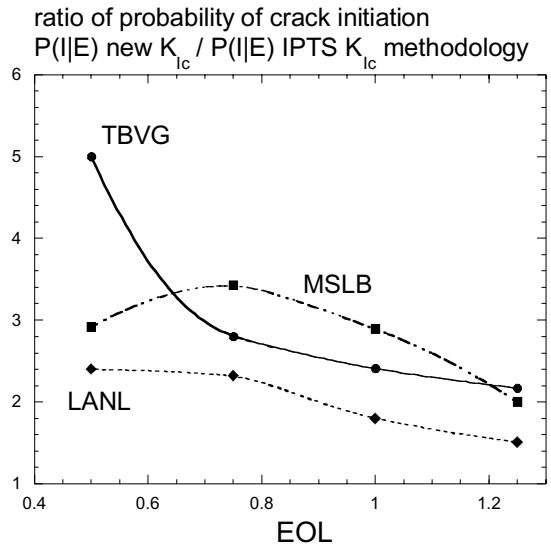

Fig. 20. Ratio of *P(I|E)*s computed in applications of the ORNL and IPTS K_{Ic} models to Oconee dominant PTS transients.

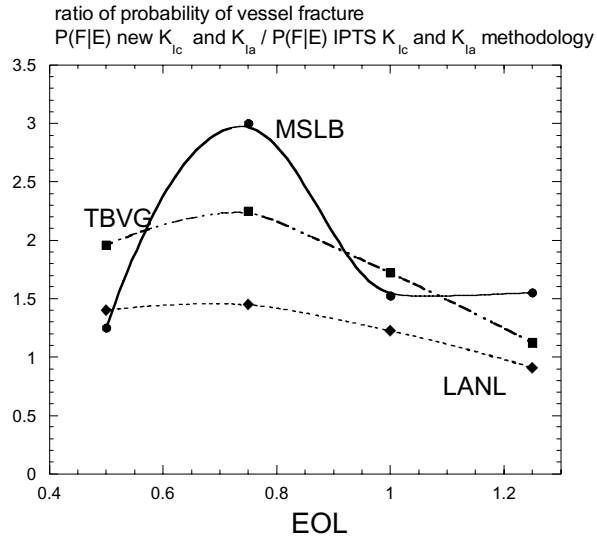

Fig 21. Ratio of *P(F|E)*s computed in applications of the ORNL and IPTS K_{Ic} and K_{Ia} models to Oconee dominant PTS transients.

Internal Distribution

1-5. B. R. Bass
6. K. O. Bowman
7. W. G. Craddick
8. K. W. Childs
9. T. L. Dickson
10. D. M. Hetrick
11. M. A. Kuliasha
12. S. K. Iskander
13. W. J. McAfee
14. R. K. Nanstad
15-16. C. E. Pugh
17. T. M. Rosseel
18. J. J. Simpson
19. M. A. Sokolov
20-24. P. T. Williams
25. Laboratory Records

External Distribution

26. W. H. Bateman, NRR, U.S. Nuclear Regulatory Commission, MS O7 D4, Washington, D.C. 20555-0001
27. R. H. Dodds, 3140 Newmark Laboratory, 205 North Matthews, Urbana, IL 61801
28. C. J. Fairbanks, RES/DET/MEB, U.S. Nuclear Regulatory Commission, MS T-10 E10, Washington, D.C. 20555-0001
29. E. M. Hackett, RES/DET/MEB, U.S. Nuclear Regulatory Commission, MS T-10 E10, Washington, D.C. 20555-0001
30. J. A. Joyce, U.S. Naval Academy, Mechanical Engineering Department, MS 11C, 590 Hollway Road, Annapolis, MD 21402
31-35. M. T. Kirk, RES/DET/MEB, U.S. Nuclear Regulatory Commission, MS T-10 E10, Washington, D.C. 20555-0001
36-37. S. N. Malik, RES/DET/MEB, U.S. Nuclear Regulatory Commission, MS T-10 E10, Washington, D.C. 20555-0001
38. M. E. Mayfield, RES/DET, U.S. Nuclear Regulatory Commission, MS T-10 E10, Washington, D.C. 20555-0001
39. M. A. Mitchell, NRR, U.S. Nuclear Regulatory Commission, MS O7 D4, Washington, D.C. 20555-0001
40. M. Modarres, University of Maryland, Center for Reliability Engineering, College Park, MD 20742
41. A. Mosleh, Materials and Nuclear Engineering Dept., University of Maryland, 2100A Marie Mount Hall, College Park, MD 20742-7531
42. M. E. Natishan, Materials Characterization Laboratory, A. J. Clarke School of Engineering, University of Maryland, College Park, MD 20742
43. C. G. Santos, RES/DET/MEB, U.S. Nuclear Regulatory Commission, MS T-10 E10, Washington, D.C. 20555-0001
44. W. J. Shack, Energy Technology Division, Argonne National Laboratory, 9700 S. Cass Avenue, Argonne, IL 60439
45. N. O. Siu, RES/DRAA, U.S. Nuclear Regulatory Commission, MS T-10 E50, Washington, D.C. 20555-0001
46. R. L. Tregoning, Fatigue and Fracture Branch, Carderock Division, Naval Surface Warfare Center, 9500 McArthur Blvd., West Bethesda, MD 20817-5700
47. K. R. Wichman, NRR, U.S. Nuclear Regulatory Commission, MS O7 D4, Washington, D.C. 20555-0001